Biogeosciences Discuss., 6, 11127–11157, 2009
www.biogeosciences-discuss.net/6/11127/2009/

Biogeosciences Discussions

This discussion paper is/has been under review for the journal Biogeosciences (BG).
Please refer to the corresponding final paper in BG if available.

Individual and interacting effects of pCO_2 and temperature on *Emiliania huxleyi* calcification: study of the calcite production, the coccolith morphology and the coccosphere size

C. De Bodt[1], N. Van Oostende[2], J. Harlay[1,*], K. Sabbe[2], and L. Chou[1]

[1]Laboratoire d'Océanographie Chimique et Géochimie des Eaux, Université Libre de Bruxelles (ULB), Belgium
[2]Protistology & Aquatic Ecology, Gent University (UGent), Belgium
[*]now at: Unité d'Océanographie Chimique – Université de Liège (ULg), Belgium

Received: 4 November 2009 – Accepted: 10 November 2009 – Published: 27 November 2009

Correspondence to: C. De Bodt (cdebodt@ulb.ac.be)

Published by Copernicus Publications on behalf of the European Geosciences Union.

Abstract

The impact of ocean acidification and increased water temperature on marine ecosystems, in particular those involving calcifying organisms, has been gradually recognised. We examined the individual and combined effects of increased pCO_2 (180 ppm V CO_2, 380 ppm V CO_2 and 750 ppm V CO_2 corresponding to past, present and future CO_2 conditions, respectively) and temperature (13°C and 18°C) during the calcification phase of the coccolithophore *E. huxleyi* using batch culture experiments. We showed that the cell abundance-normalized particulate organic carbon concentration (POC) increased from the present to the future CO_2 treatments. A significant effect of pCO_2 and of temperature on calcification was found, manifesting itself in a lower cell abundance-normalized particulate inorganic carbon (PIC) content as well as a lower PIC:POC ratio at future CO_2 levels and at 18°C. Coccosphere-sized particles showed a size reduction trend with both increasing temperature and CO_2 concentration. The influence of the different treatments on coccolith morphology was studied by categorizing SEM coccolith micrographs. The number of well-formed coccoliths decreased with increasing pCO_2 while temperature did not have a significant impact on coccolith morphology. No interacting effect of pCO_2 and temperature was observed on calcite production, coccolith morphology or on coccosphere size. Finally, our results suggest that ocean acidification might have a larger adverse impact on coccolithophorid calcification than surface water warming.

1 Introduction

The global atmospheric carbon dioxide (CO_2) concentration increased from a pre-industrial value of about 280 ppm V to 379 ppm V in 2005 (IPCC, 2007). The anthropogenic gas emissions have led to a rise by 0.74±0.18°C in global average surface temperature from 1906 to 2005 (IPCC, 2007). One fourth of the CO_2 emitted to the atmosphere is absorbed by the ocean (Canadell et al., 2007) where CO_2 dissolves in

BGD

6, 11127–11157, 2009

the surface waters, decreasing the seawater pH, the availability of carbonate ions, and the saturation state of seawater with respect to calcium carbonates (Ω_{cal}) (Zeebe and Wolf-Gladrow, 2001). Global warming results in an enhancement in vertical stratification of the water column, leading therefore to a decreased mixing between the surface ocean and the deeper layers with a consequent decrease in the supply of nutrients (Bopp et al., 2001) and dissolved inorganic carbon (DIC) (Borges et al., 2008). Increasing stratification results also in a shoaling of the upper mixed layer leading to an increase in the light availability in this layer (Bopp et al., 2001).

Both ocean acidification and warming influence the distribution of DIC for calcifying organisms and therefore have the potential to alter the particulate inorganic and/or organic carbon production, which would affect the efficiency of particle export. By photosynthesis in the photic zone, phytoplankton draws down CO_2:

$$16CO_2 + 16NO_3^- + H_2PO_4^- + 17H^+ + 122H_2O \leftrightarrow (CH_2O)_{106}(NH_3)_{16}H_3PO_4 + 138O_2 \quad (1)$$

In contrast, biogenic calcification releases CO_2:

$$Ca^{2+} + 2HCO_3^- \rightarrow CaCO_3 + CO_2 + H_2O \quad (2)$$

The biological carbon pump could thus remove particulate carbon from the euphotic zone by exporting it to the oceanic interior. Ballast minerals such as biogenic calcite ($CaCO_3$) enhance the flux of organic carbon from the surface ocean to the ocean floor (Armstrong et al., 2002; François et al., 2002; Klaas and Archer, 2002). The rain ratio, defined here as the ratio of particulate inorganic carbon (PIC) to particulate organic carbon (POC) in exported biogenic matter, determines the relative strength of the biological carbon pump and consequently the flux of CO_2 across the surface ocean–atmosphere interface.

The effect of higher pCO_2 on benthic or pelagic calcifying organisms is well documented in literature (for corals: Gattuso et al., 1998; Kleypas et al., 1999; for foraminifera: Spero et al., 1997; Bijma et al., 1999; for the coccolithophore *Emiliania huxleyi*: Riebesell et al., 2000; Zondervan et al., 2001, 2002; Sciandra et al., 2003;

BGD
6, 11127–11157, 2009

Delille et al., 2005; Engel et al., 2005). These studies indicated a decrease of calcification in response to an increase of CO_2. However, Langer et al. (2006) showed that this observation was not so straightforward: two species of coccolithophores, *Coccolithus pelagicus* and *Calcidiscus leptoporus*, did not exhibit the same response to increasing CO_2. Compared to cultures of *E. huxleyi*, PIC production in *C. pelagicus* cultures did not change with increasing CO_2, while *C. leptoporus* showed an optimum production of PIC at present CO_2 conditions. The authors suggested a species-specific response. In contrast to previous laboratory and field experiments involving *E. huxleyi*, Iglesias-Rodriguez et al. (2008a) showed an increase in calcification with increasing pCO_2. The response of *E. huxleyi* to increasing CO_2 levels is therefore still a matter of debate (e.g. Riebesell et al., 2008; Iglesias-Rodriguez et al., 2008b).

Only few studies to date have tested the combined effect of increased pCO_2 and temperature on calcification, which are likely to be relevant in natural settings (for corals: Reynaud et al., 2003; for coccolithophores: Feng et al., 2008). An interacting effect of pCO_2 and temperature was found for the scleractinian coral *Stylophora pistillata*, with a 50% reduction in calcification when both parameters increased (Reynaud et al., 2003). Feng et al. (2008) demonstrated a decrease in cellular PIC from 375 ppm V to 750 ppm V CO_2 (a decrease by 50% at 20°C and by 41% at 24°C) for *E. huxleyi* cultured at high light intensities (400 μmol photons m^{-2} s^{-1}), but did not observe a significant effect of temperature on calcification.

In this study we used batch culture of the coccolithophore *E. huxleyi* grown under different conditions of pCO_2 and temperature to assess the effect of simulated ocean acidification and warming on calcification and cell size. To this end, we examined the individual and combined effects of increased pCO_2 (180 ppm V CO_2, 380 ppm V CO_2 and 750 ppm V CO_2 corresponding to past, present and future CO_2 conditions, respectively) and temperature (13°C and 18°C) on the POC and PIC productions, the PIC:POC ratio, the coccosphere size spectrum, and the coccolith morphology.

BGD
6, 11127–11157, 2009

2 Materials and methods

2.1 Experimental set-up and sampling

Duplicate laboratory experiments were performed on monospecific batch cultures of *E. huxleyi* (strain AC481 from Normandy, France, Algobank-Caen microalgal collection) at different pCO_2 corresponding to glacial, present and year 2100 atmospheric CO_2 concentrations by bubbling gases at fixed CO_2 concentrations (respectively 180±8 ppm V "low CO_2", 379±11 ppm V "present CO_2" and 740±16 ppm V "future CO_2" (Air Liquide, Belgium)). Experiments were carried out in 2 temperature-controlled incubators, under low, present and future CO_2 conditions at 13°C and under present and future CO_2 conditions at 18°C. Cells were acclimated to the experimental conditions for 10 days (d) to avoid measuring potential adaptation effects during the dedicated experiments. The culture medium consisted of filtered (0.2 μm) and autoclaved aged surface post-bloom seawater sampled in the northern Atlantic Ocean (47°45′ N, 7°00′ W), enriched with nitrates and phosphates to obtain final concentrations of 32 μmol L^{-1} and 1 μmol L^{-1}, respectively. Incident photon flux density was 150 μmol m^{-2} s^{-1} and the light/dark cycle was 14 h/10 h. Cultures (8 L) were inoculated with pre-adapted cells in exponential growth phase and were grown in 10-L sized polycarbonate carboys (Nalgene). Bloom development was monitored for a period of 44 to 57 d, encompassing the exponential and the stationary growth phase. Time is referred as d_x with x as the number of days after inoculation. Samples were taken with a sterile syringe always at the same time in the light cycle. In vivo fluorescence and turbidity (Turner fluorometer-turbidimeter) were measured daily and were used as an indicator for phytoplankton growth and calcification, respectively. Chlorophyll-*a* (chl-*a*), cell density, POC and PIC were measured every two or three days depending on the growth phase of the culture. Additional samples for scanning electron microscopy (SEM) and particle size measurement were taken as well.

BGD
6, 11127–11157, 2009

2.2 Growth parameters of *E. huxleyi*

Chl-*a* concentration was determined following the fluorometric method of Yentsch and Menzel (1963). Forty milliliter samples were filtered through GF/F filters under low vacuum. Filters were stored in the dark at −20°C until analysis. For the analysis, the filters were extracted with 10 mL of 90% acetone at −20°C overnight. Samples were then centrifuged (10 min, 4250×g) and the fluorescence of the extract was measured with a Shimadzu RF-150 fluorometer, using an excitation wavelength of 430 nm and an emission wavelength of 663 nm. The fluorescence was calibrated with a stock solution of pure chl-*a* (Merck).

Cell densities were estimated by haemocytometer counting (Malassez cell) using a light microscope. Light microscopy also permitted a visual check of the health status of the culture. The net specific growth rate (μ) was calculated for each treatment as the average of the daily growth rates during the cell growth phase:

$$\mu_x = [\ln(C_x) - \ln(C_{x-1})]/[t_x - t_{x-1}], \quad (3)$$

where $\ln(C_x)$ and $\ln(C_{x-1})$ are the natural logarithms of cell concentrations on two consecutive days.

POC concentration (in mg C L^{-1}) was measured using a Fisons NA-1500 elemental analyzer. For this analysis, 40 mL of water were filtered through pre-combusted (4 h, 500°C) GF/F filters. The measurements were carried out on the filters after the removal of carbonates by overnight exposure to strong hydrochloride acid (HCl) fumes. Calibration of the analyzer was performed using certified reference stream sediment (STSD-2) from the Geological Survey of Canada.

2.3 Calcification of *E. huxleyi*

PIC concentration (in mg C L^{-1}) was measured using a Fisons NA-1500 elemental analyzer. As for the POC analysis described above, 40 mL of water was filtered through

BGD
6, 11127–11157, 2009

pre-combusted (4 h, 500°C) GF/F filters and total particulate carbon (TPC) was measured on the filters. PIC was determined by subtracting POC from TPC. The daily rate of calcification was calculated as $\Delta PIC/\Delta t$.

Total alkalinity (TA) was measured by potentiometric titration with HCl (0.1 N, Merck) using the classical Gran procedure (Gran, 1952). Data were quality checked by analysis of Certified Reference Material (A. Dickson, CDIAC). TA was corrected for nitrate and phosphate consumption according to the equation of photosynthesis of Redfield et al. (1963) (Eq. 1), using the following relation:

$$TA = TA_{measured} - \Delta NO_3^- - \Delta H_2PO_4^- \quad (4)$$

where ΔNO_3^- and $\Delta H_2PO_4^-$ denote the nitrate and the phosphate consumed since the beginning of the experiment (d_0) (Delille et al., 2005).

TA of the seawater is affected in addition by calcification (or dissolution) because the precipitation of 1 mole of $CaCO_3$ reduces the TA by 2 moles (Eq. 2). $CaCO_3$ concentration (in μmol $CaCO_3$ kg^{-1} SW) could then be calculated from changes in TA using the alkalinity anomaly technique (Smith and Key, 1975; Chisholm and Gattuso, 1991):

$$\left[CaCO_3\right]_x = -1/2 \times (TA_x - TA_0), \quad (5)$$

where TA_x is the alkalinity on day x and TA_0 is the initial alkalinity, both corrected for nutrient consumption.

2.4 Coccolith morphology

For scanning electron microscopic analyses, 1 mL of sample was concentrated onto a polycarbonate Nuclepore (0.4 μm pore-size) filter. The filters were dried overnight at 50°C, and stored dry at room temperature until analysis. The filters were fitted onto glass microscope slides with conductive glue and then sputter-coated with gold (JFC 1200, Jeolscan). Digital images of coccospheres were acquired using a Jeolscan SEM (JSM 5600 LV) and examined at a magnification of at least 8000×.

BGD
6, 11127–11157, 2009

A minimum of 100 coccoliths (attached onto the coccosphere) were analyzed per CO_2 and temperature treatment duplicate. Only about 2 coccoliths per coccosphere were exposed in the right way to allow categorization, so at least 50 coccospheres were analyzed. SEM images were analyzed on d_{20}, at the end of the exponential growth phase. Categorization of attached coccoliths was preferred to loose coccoliths of unknown age and dissolution status. Coccoliths were visually classified according to four categories (Fig. 1). The first category corresponds to normal coccoliths with all segments connected and forming an oval ring. The next three categories represent stages of increasing malformation. The second one corresponds to slightly malformed coccoliths; in this category less than 5 T-segments are not well connected to others. The third category corresponds to malformed coccoliths where more than 5 T-segments are unconnected or not entirely formed. The fourth one corresponds to fragmented coccoliths; in this category parts of the coccolith are missing.

2.5 Coccosphere size frequency distribution

Size distribution of particles was determined with a Beckman Coulter Counter (Coulter Multisizer III). For each experimental treatment and for both replicates, 3 sampling time points situated around the chlorophyll maximum of the cultures were analyzed. Fixed samples (3% borate-buffered, 0.2 μm filtered, formaldehyde solution) were measured using a 50 μm aperture tube. Particle size measurements were calibrated using 10 μm latex microspheres (NIST). Particles between 2 μm and 10 μm equivalent spherical diameter (ESD) were binned into 256 size classes. Only the particles between 3.5 μm and 7 μm ESD, corresponding to the *E. huxleyi* coccosphere size range, were further analyzed. An average of 5735 coccosphere-sized particles (CSP) were analyzed per sample. For statistical tests, the mean particle size of CSP of each replicate was used. The volume of CSP was calculated based on that of a sphere.

BGD
6, 11127–11157, 2009

2.6 Statistical treatment of data

The average value of parameters from duplicate cultures is given as the statistical mean (x) together with the minimum and maximum value (x [min; max]). Mean values were compared by means of a Student's t-test. Analysis of the effect of the pCO_2 and/or temperature treatment on a linear relationship between two variables was carried out by comparing the slope of the significant linear regression, calculated for each treatment separately. The influence of the CO_2 treatment on variables was determined by means of a one-way analyses of variance (ANOVA) or a t-test. A two-way ANOVA was used to determine the statistical significance of the effect of pCO_2 (present and future CO_2 conditions) and temperature (13°C and 18°C) treatments and their interaction. To assess if the qualitative differences in coccolith morphology between temperature or pCO_2 treatments were statistically significant, either the non-parametric Mann-Whitney U test or the Kruskal-Wallis test was used, respectively. All statistical treatments of data were done with GraphPad Prism (version 5).

3 Results

3.1 Bloom development of *E. huxleyi* during the culture experiments

The increase in chl-*a* corresponded to the beginning of the exponential growth phase (Fig. 2a). Maximum chl-*a* concentration varied between cultures from 7.3 to 19.6 $\mu g\,L^{-1}$ and was generally observed on around d_{20}. This peak corresponded to PO_4 depletion (data not shown). The duration of the exponential growth phase varied between 7 (low CO_2/13°C treatment) and 15 d (present and future CO_2/18°C treatment) from one culture experiment to another. Chl-*a* concentration then became stationary before decreasing until the end of the experiment. At 13°C, a higher maximum chl-*a* concentration was found in the future CO_2 cultures (17.3 [15.1; 19.6] $\mu g\,L^{-1}$) compared to other treatments (10.8 [9.2; 12.4] $\mu g\,L^{-1}$ in the present CO_2/13°C cultures and 10.3

BGD
6, 11127–11157, 2009

[9.8; 10.8] $\mu g\,L^{-1}$ in the low CO_2/13°C cultures) (Fig. 2a, left panel). At 18°C, the evolution of chl-*a* concentrations and the maximum concentration obtained were similar among the cultures; a maximum chl-*a* concentration of 9.2 [8.4; 10.1] $\mu g\,L^{-1}$ was reached in the future CO_2/18°C treatment and 9.1 [7.3; 10.9] $\mu g\,L^{-1}$ in the present CO_2/18°C treatment (Fig. 2a, right panel).

At 13°C, maximum cell abundance was reached between d_{36} and d_{40} for future CO_2 treatments and between d_{45} and d_{52} for the experiments at present and low CO_2 (Fig. 2b, left panel). Maximum cell densities varied from 2.22×10^5 to 3.84×10^5 cells mL^{-1} among batch cultures with highest values reached in the future CO_2 cultures (Fig. 2b, left panel). At 18°C, maximum cell density was reached between d_{34} and d_{40} depending on the experiment (Fig. 2b, right panel). In the future CO_2/18°C culture a maximum of 4.66×10^5 [4×10^5; 5.35×10^5] cells mL^{-1} was observed and 6.02×10^5 [5.2×10^5; 6.84×10^5] cells mL^{-1} in the present CO_2/18°C treatment (Fig. 2b, right panel). For the present CO_2 treatments, higher cell densities were reached in the higher temperature treatment (t-test, $p<0.05$) while no statistical difference in cell abundance was observed between the future CO_2 temperature treatments (Fig. 2b). The growth rate was calculated from the cell density for each treatment (Table 1). Growth rates were higher at 18°C than at 13°C, with an average of 0.09 d^{-1} among all cultures at 18°C and 0.06 d^{-1} at 13°C.

At 13°C, POC increased continuously from d_6 during the course of the experiment except for the low CO_2/13°C treatment where POC concentration slightly decreased from d_{34} onwards (Fig. 2c, left panel). At 13°C, maximum POC concentration varied between 1.63 mg C L^{-1} for the low and present CO_2 treatment and 3.09 mg C L^{-1} for the future CO_2 treatment (Fig. 2c, left panel). At 18°C, maximum POC concentration ranged from 4.50 to 6.02 mg C L^{-1} and concentrations were similar between the CO_2 treatments (Fig. 2c, right panel). POC production was favoured by higher growth temperatures and resulted in higher POC concentrations with bloom development in the 18°C treatments (Fig. 2c).

BGD
6, 11127–11157, 2009

3.2 Calcification in *E. huxleyi* cultures

Increases in PIC concentrations, measured with the Fisons NA-1500 elemental analyzer, could be measured from d_8 onwards in the 13°C culture experiments. Maximum PIC concentrations varied between 3.97 and 5.44 mg C L^{-1} with maximum values obtained in the future CO_2/13°C treatment (Fig. 2d, left panel). The calcification rate was higher in the future CO_2/13°C treatment with an average daily rate of 0.17 mg C L^{-1} d^{-1} in this treatment and 0.085 and 0.075 mg C L^{-1} d^{-1} in the low CO_2/13°C and present CO_2/13°C treatment, respectively (Table 1).

At 18°C, PIC concentrations increased from d_6 where maximum values ranged between 5.69 and 7.45 mg L^{-1} (Fig. 2d, right panel). Highest values were obtained more rapidly at present CO_2 with a daily rate of 0.20 mg C L^{-1} d^{-1} compared to a rate of 0.11 mg C L^{-1} d^{-1} at future CO_2/18°C (Table 1).

In both temperature treatments, variability in PIC concentrations was observed between the CO_2 treatments and within the replicates. The measured PIC concentrations agreed well with the calculated calcite concentrations derived from changes in seawater alkalinity (Fig. 3).

3.3 Effect of pCO_2 and/or temperature on the PIC and POC concentrations normalized to cell abundance

3.3.1 Cell abundance-normalized POC concentrations

POC concentration was positively correlated to *E. huxleyi* cell abundance during the cell growth phase (Table 2). As a general feature, differences in the Δ[POC]:Δ[cell] ratio were observed among the culture experiments and among duplicate.

More precisely, at 13°C significantly higher values were found in the future CO_2 treatment compared to the present CO_2 treatment (34% higher, t-test, $p<0.05$) (Fig. 4a). Furthermore, cell abundance-normalized POC levels were higher in the low CO_2/13°C compared to present CO_2/13°C treatment by 19%.

BGD
6, 11127–11157, 2009

At 18°C, higher values were found in the future compared to the present CO_2 treatment, although this difference was not statistically significant due to elevated standard deviations per treatment (Table 2).

A two-way ANOVA indicated a significant effect of the pCO_2 ($p<0.005$) on the Δ[POC]:Δ[cell] ratio, while neither the effect of the temperature nor the interacting effect of pCO_2 and temperature on this ratio were significant ($p=0.1208$ and 0.5755, respectively).

3.3.2 Cell abundance-normalized PIC concentrations

The PIC was linearly correlated to the abundance of *E. huxleyi* when Ω_{cal} was higher than 1 (Table 2).

At 13°C, the highest cell abundance-normalized PIC ratio was found in the low CO_2 treatment and was significantly different from the present CO_2 treatment (by 19%) or from the future CO_2 treatment (by 46%) (t-test, $p<0.05$) (Fig. 4b). However, no significant difference was found between the low CO_2/13°C and the present CO_2/13°C treatments (t-test, $p=0.09$). Nevertheless, a one-way ANOVA indicated a significant effect of the pCO_2 ($p<0.05$) with a decrease in the Δ[PIC]:Δ[cell] ratio with increasing pCO_2 at 13°C.

At 18°C, the ratio was lower in the future CO_2/18°C than in the present CO_2/18°C but the difference was not significant (t-test, $p=0.75$).

The ratio Δ[PIC]:Δ[cell] decreased with temperature, by 34% at present CO_2 and by 7% at future CO_2.

Both pCO_2 and temperature had a significant effect on the Δ[PIC]:Δ[cell] ratio in the present and future CO_2 treatments (two-way ANOVA, $p<0.05$ and $p<0.05$, respectively), although no significant interaction was found between both variables ($p=0.06$).

BGD
6, 11127–11157, 2009

3.3.3 PIC:POC ratio

Like cell abundance-normalized PIC, the PIC:POC ratio was lower in the future CO_2/13°C treatment than in the present or in the low CO_2/13°C treatment by 42% and 41%, respectively (one-way ANOVA, $p<0.05$, Fig. 4c).

At 18°C, the PIC:POC ratio was lower in the future than in the present CO_2 treatment by 29% (t-test, $p<0.05$).

With an increase in temperature, the ratio decreased by 23% in the present CO_2 treatment and by 7% in the future CO_2 treatment.

No interactive effect of pCO_2 and the temperature was found (two-way ANOVA, $p=0.09$) but a significant effect of the pCO_2 ($p<0.0001$) and of the temperature ($p<0.05$) on the PIC:POC ratio was found.

3.4 Coccolith morphology

SEM analysis revealed variable degrees of coccolith malformation. A significant effect of the CO_2 treatments on coccolith morphology was found at 13°C (Kruskal-Wallis test, $p<0.0001$) as well as at 18°C (Mann-Whitney U test, $p<0.0001$) while temperature did not significantly affect coccolith morphology (Mann-Whitney U test, $p_{present}=0.4090$, $p_{future}=0.1915$) (Fig. 5). The percentage of normal coccoliths was more important in the cultures with low CO_2/13°C conditions (43%) than at present CO_2 condition with 22% in the 13°C and 29% in the 18°C treatment. Finally, the lowest percentage of normally formed coccoliths was observed in the future CO_2 treatments, with 13% and 9% at 13°C and 18°C, respectively. The percentage malformed coccoliths increased with increasing pCO_2, with 23% and 28% of fragmented coccoliths observed in the future CO_2/13°C and 18°C treatment, respectively, while only 7% of the coccoliths were fragmented in the low CO_2/13°C experiment.

BGD
6, 11127–11157, 2009

3.5 Coccosphere size frequency distribution

The mean particle size of CSP was significantly different between the different CO_2 and temperature treatments (ANOVA, $p<0.0001$) (Fig. 6). A clear trend in CSP ESD reduction was observed with increasing pCO_2 and temperature conditions. The mean particle size of CSP was significantly smaller at 18°C than at 13°C ($t\text{-test}_{present-future}$, $p<0.05$). Differences in mean particle size of CSP were also found among the CO_2 treatments ($ANOVA_{13°C}$, $p<0.0001$, $t\text{-test}_{18°C}$, $p<0.05$), with CSP smaller in future CO_2 than in the present CO_2treatments ($t\text{-test}_{13°C-18°C}$, $p<0.05$) but CSP not significantly smaller in the present day CO_2 treatment than in low CO_2 conditions ($t\text{-test}_{13°C}$, $p=0.0897$). Temperature did not significantly exacerbate the effect of CO_2 on the mean CSP size (two-way ANOVA, $p=0.8261$).

4 Discussion

In this study, the bloom development of *E. huxleyi* was followed from the beginning of the exponential growth phase. As a general feature in culture experiments, chl-*a* concentration and the particulate component increased while nutrients were consumed, reaching a stationary phase where PO_4 became depleted and chl-*a* levels slowly decreased while POC and PIC accumulated. This evolution was monitored in cultures subjected to different treatments of pCO_2 and temperature to assess the effect of ocean acidification and global warming on the organic and inorganic carbon production of *E. huxleyi*.

The chl-*a* content to the volume of coccosphere ($V=\pi[ESD]^3/6$) ratio is not significantly different between treatments (t-test, $p=0.0868$). However, higher chl-*a* concentration and lower cell density were observed at 13°C compared to 18°C (Fig. 2). The smaller size of coccosphere at 18°C (Fig. 6) is likely to be at the origin of the lower chl-*a* per cell ratio at higher temperature.

In all treatments, a delay between the onset of the POC and the PIC production

BGD
6, 11127–11157, 2009

was observed. This delay was longer for the cultures at 18°C (5 d) than at 13°C (2 d). Such a delay has already been observed by Delille et al. (2005) and De Bodt et al. (submitted), where this delay was shown to increase with increasing pCO_2, in disagreement with the results of the present study. This difference could be ascribed to the acclimation of the algal cells to pCO_2 and temperature conditions used in our future experimental treatment while neither in De Bodt et al. (submitted) nor in the mesocosm experiment (Delille et al., 2005) acclimation was carried out.

4.1 Impact of increasing pCO_2/temperature on the Δ[POC]:Δ[cell] ratio

An increase in the Δ[POC]:Δ[cell] ratio was observed in the future CO_2 compared to the present CO_2 treatment (at 13°C and 18°C), but a higher ratio was also found in the low compared to the present CO_2 treatment (at 13°C). No clear effect of the pCO_2 was observed here for the Δ[POC]:Δ[cell] ratio and previous studies also showed contradictory results. In batch culture experiments, an increase in the POC production (Riebesell et al., 2000; Zondervan et al., 2001) is generally observed with increasing CO_2 levels while in mesocosm experiments no significant changes are observed (Delille et al., 2005). Nevertheless, a higher loss of POC in the future CO_2 mesocosm was obtained. While the growth rate was more important at 18°C than at 13°C, no significant effect of temperature was observed on the cellular POC content.

Nevertheless, in some treatments corresponding to future conditions (future CO_2/13°C, present CO_2/18°C, future CO_2/18°C), higher POC concentrations than expected from the Redfield stoichiometry were measured. Indeed, a consumption of 32 μmol L^{-1} of nitrates induces a production of 212 μmol L^{-1} of POC (or 2.5 mg L^{-1} POC). This suggests the occurrence during these experiments of carbon overconsumption, which refers to a continuous uptake of DIC by phytoplankton after nutrient exhaustion (Banse, 1994). Carbon overconsumption could lead to the exudation of carbon-rich dissolved organic matter (DOM) which can aggregate to form extracellular particulate organic matter (POM) (Schartau et al., 2007). This implies an increase in extracellular release of primary production at the expense of cellular biomass due to

BGD
6, 11127–11157, 2009

increased CO_2 levels.

4.2 Impact of increasing CO_2/temperature on the Δ[PIC]:Δ[cell] ratio

The cell abundance-normalized PIC levels decreased with increasing pCO_2 and a reduction by 34% in the Δ[PIC]:Δ[cell] ratio was measured between the present and the future CO_2 treatment at 13°C. While the different pCO_2 conditions were simulated by bubbling gases at fixed CO_2 concentrations, we obtained similar results to Riebesell et al. (2000) and Zondervan et al. (2001) who modified the pCO_2 by the addition of acid/base instead. The effect of increasing pCO_2 on *E. huxleyi* is rather well studied and it is generally accepted that calcification decreases with increasing pCO_2, although the study of Iglesias-Rodriguez et al. (2008a) showed contradicting results.

Rost et al. (2008) encouraged studies manipulating multiple environmental factors to assess their interactive effects. In addition to the pCO_2, we also investigated the effect of temperature on bloom variables. The calcification per cell decreased from the present CO_2/13°C to the future CO_2/18°C treatment by 37%, yet no significant interacting effect of pCO_2 and temperature on calcification was found. Increasing the temperature by 5°C decreased the calcification per cell by 34% in the culture at present CO_2 and by 7% in the one at future CO_2. The latter result was not corroborated by Feng et al. (2008) who also studied the interactive effect of pCO_2 (375 ppm V and 750 ppm V) and temperature (20 and 24°C) at two different irradiances (50 and 400 μmol m^{-2} s^{-1}) using semi-continuous laboratory cultures. As in our study, these authors observed a reduction in the cell abundance-normalized PIC with increasing pCO_2, but only at high irradiance (400 μmol m^{-2} s^{-1}). Lower PIC levels at high pCO_2 could be explained by: (1) a lower calcite content per coccolith (2) a decrease in coccolith number per coccolithophore cell or (3) a decrease in coccolith production rate, all of them not mutually exclusive. Our data suggest, however, a reduction in the number of coccoliths per cell indicated by the fact that cells were smaller under future CO_2 conditions. In addition, SEM examinations of coccolith morphology point towards a lower calcite content per

BGD
6, 11127–11157, 2009

coccoliths at high pCO_2.

4.3 Impact of increasing CO_2/temperature on the coccosphere size

A decrease in the mean size of CSP with increasing temperature and CO_2 conditions was observed, suggesting either a biovolume reduction or a decrease in coccolith cell coverage. Coulter size measurements are based on the measurement of the electrical signal generated by displacement of an electrolyte volume and thus no differentiation can be made between the share of biovolume and coccoliths making up the coccosphere. A reduction in the mean coccosphere volume by 10% (±1%) was observed across treatments with increasing pCO_2. This result is in accordance with Engel et al. (2005) who found lower coccosphere size at high CO_2 concentrations.

Cell volume in protists is known to decrease while cell division increases with increasing temperature (Montagnes and Franklin, 2001; Atkinson et al., 2003). Here, we noted a decrease in coccosphere volume of 3% per °C (present and future CO_2 treatments), which is in accordance with the values for biovolume reduction proposed by Atkinson et al. (2003). With increasing temperature, the growth rate increased while a decrease in cell size in parallel to a decrease in calcification was observed and the effect of temperature was more important at present than at future pCO_2. Sorrosa et al. (2005) also found that a higher growth temperature would induce a reduction in cell size and intracellular calcification in *E. huxleyi*.

4.4 Impact of increasing CO_2/temperature on the coccolith morphology

In parallel to the decrease in Δ[PIC]:Δ[cell] ratio with increasing pCO_2, an increased share of abnormal coccoliths was observed in our experiments. In addition, the cellular calcification rate (expressed in pmol PIC cell^{-1} d^{-1}) decreased while the percentage of aberrant coccoliths increased, suggesting that the decrease in PIC cell^{-1} was due to altered calcite content per coccoliths (Fig. 7). Changes in PIC production have already been associated with alterations of coccolith morphology (Langer et al., 2006).

BGD
6, 11127–11157, 2009

Riebesell et al. (2000) have also documented *E. huxleyi* cells with deformed coccoliths or an incomplete coccosphere in high pCO_2 cultures. Contrary to our results, Iglesias-Rodriguez et al. (2008a) observed an increase in the PIC production with increasing pCO_2 associated with an increase in the coccolith size. While no effect of temperature on coccolith morphology could be detected in our study, Watabe and Wilbur (1966) found that the percentage of abnormal coccolith increased at lower and higher temperature extremes (cultures at 7, 12, 18, 24 and 27°C). Our temperature range may be too small to observe such an effect.

5 Conclusions

In the light of our experimental results, *E. huxleyi* is sensitive to changes in pCO_2 and temperature. Coccosphere-sized particles showed a size reduction trend with both increasing temperature and pCO_2 concentration. The ratio of the PIC concentration per cell was shown to be lower at future CO_2/18°C. This could lead to a smaller ballast effect and thus a reduction in C export as highlighted by a lower PIC:POC rain ratio.

A lower PIC:cell ratio can thus be expected under future pCO_2 conditions, which is reflected by the deteriorated coccolith morphology measured in our culture experiments, while no significant effect of temperature on the coccolith morphology was observed. The sole future increase in pCO_2 may thus have a larger adverse impact on the calcification of *E. huxleyi* than the increase in temperature alone or the interacting effect of temperature and pCO_2.

Acknowledgement. N. Roevros is gratefully acknowledged for her technical assistance in the laboratory. We would like to thank A. Borges, B. Delille and K. Suykens from the University of Liège for their assistance in the measurements of pH and DIC and for their fruitful comments. C. De Bodt was supported by a PhD grant from the EU FP6 IP CarboOcean project (contract no. 511176–2). N. Van Oostende received a PhD grant from the Institute for the Promotion of Innovation through Science and Technology in Flanders (IWT-Vlaanderen). This study was also funded by Belgian Federal Science Policy Office in the framework of the PEACE project (con-

tract numbers SD/CS/03A and SD/CS/03B). It is also a contribution to the EU FP7 IP EPOCA project (contract no. 211384). The present work is a Belgian contribution to the international SOLAS project.

References

Armstrong, R. A., Lee, C., Hedges, J. I., Honjo, S., and Wakeham, S. G.: A new, mechanistic model for organic carbon fluxes in the ocean based on the quantitative association of POC with ballast minerals, Deep-Sea Res., 49, 219–236, 2002.

Atkinson, D. A., Ciotti, B. J., and Montagnes, D. J. S.: Protists decrease in size linearly with temperature: ca. 2.5% $^{\circ}C^{-1}$, Philos. T. Roy. Soc. B, 270, 2605–2611, 2003.

Banse, K.: Uptake of inorganic carbon and nitrate by marine plankton and the Redfield ratio, Global Biogeochem. Cy., 8, 81–84, 1994.

Bijma, J., Spero, H. J., and Lea, D. W.: Reassessing Foraminiferal Stable Isotope Geochemistry: Impact of the Oceanic Carbonate System (Experimental Results), in: Use of Proxies in Paleoceanography: Examples from the South Atlantic, edited by: Fischer, G. and Wefer, G., Springer-Verlag, Berlin Heidelberg, 489–512, 1999.

Bopp, L., Monfray, P., Aumont, O., Dufresne, J.-L., Le Treut, H., Madec, G., Terray, L., and Orr, J. C.: Potential impact of climate change on marine export production, Global Biogeochem. Cy., 15, 81–99, 2001.

Borges, A. V., Tilbrook, B., Metzl, N., Lenton, A., and Delille, B.: Inter-annual variability of the carbon dioxide oceanic sink south of Tasmania, Biogeosciences, 5, 141–155, 2008, http://www.biogeosciences.net/5/141/2008/.

Canadell, J. G., Le Quéré, C., Raupach, M. R., Field, C. B., Buitenuis, E. T., Ciais, P., Conway, T. J., Gillett, N. P., Houghton, R. A., and Marland, G.: Contributions to accelerating atmospheric CO_2 growth from economic activity, carbon intensity, and efficiency of natural sinks, P. Natl. Acad. Sci. USA, 104, 18866–18870, 2007.

Chisholm, J. R. M. and Gattuso, J.-P.: Validation of the alkalinity anomaly technique for investigating calcification and photosynthesis in coral reef communities, Limnol. Oceanogr., 36, 1232–1239, 1991.

De Bodt, C., Harlay, J., d'Hoop, Q., and Chou, L.: Calcification and transparent exopolymer particles (TEP) production in batch cultures of *Emiliania huxleyi*, submitted, 2009.

Delille, B., Harlay, J., Zondervan, I., Jacquet, S., Chou, L., Wollast, R., Bellerby, R. G. J., Frankignoulle, M., Borges, A. V., Riebesell, U., and Gattuso, J.-P.: Response of primary production and calcification to changes of pCO_2 during experimental blooms of the coccolithophorid *Emiliania huxleyi*, Global Biogeochem. Cy., 19, GB2023, doi:10.1029/2004GB002318, 2005.

Engel, A., Zondervan, I., Aerts, K., Beaufort, L., Benthien, A., Chou, L., Delille, B., Gattuso, J.-P., Harlay, J., Heemann, C., Hoffmann, L., Jacquet, S., Nejstgaard, J., Pizay, M.-D., Rochelle-Newall, E., Schneider, U., Terbrueggen, A., and Riebesell, U.: Testing the direct effect of CO_2 concentration on a bloom of the coccolithophorid *Emiliania huxleyi* in mesocosm experiments, Limnol. Oceanogr., 50, 493–507, 2005.

Feng, Y., Warner, M. E., Zhang, Y., Sun, J., Fu, F.-X., Rose, J. M., and Hutchins, D. A.: Interactive effects of increased pCO_2, temperature and irradiance on the marine coccolithophore *Emiliania huxleyi* (Prymnesiophyceae), Eur. J. Phycol., 43, 87–98, 2008.

François, R., Honjo, S., Krishfield, R. A., and Manganini, S. J.: Factors controlling the flux of organic carbon to the bathypelagic zone of the ocean, Global Biogeochem. Cy., 16, 1–19, 2002.

Gattuso, J.-P., Frankignoulle, M., Bourge, I., Romaine, S., and Buddemeier, R. W.: Effect of calcium carbonate saturation of seawater on coral calcification, Global Planet. Change, 18, 37–46, 1998.

Gran, G.: Determination of the equivalence point in potentiometric titrations. Part II, Analyst, 77, 661–671, 1952.

Iglesias-Rodriguez, M. D., Halloran, P. R., Rickaby, R. E. M., Hall, I. R., Colmenero-Hidalgo, E., Gittins, J. R., Green, D. R. H., Tyrrel, T., Gibbs, S. W., von Dassow, P., Rehm, E., Armbrust, E. V., and Boessenkool, K. P.: Phytoplankton calcification in a high-CO_2 world, Science, 320, 336–340, 2008a.

Iglesias-Rodriguez, M. D., Buitenhuis, E. T., Raven, J. A., Schofield, O., Poulton, A. J., Gibbs, S., Halloran, P. R., and de Baar, H. J. W.: Response to comment on "Phytoplankton calcification in a high-CO_2 world", Science, 322, 1466c, doi:10.1126/Science.1161501, 2008b.

IPCC: Climate Change 2007: Synthesis Report. Contribution of Working Groups I, II and III to the Fourth Assessment Report of the Intergovernmental Panel on Climate Change, edited by: Core Writing Team, Pachauri, R. K. and Reisinger, A., IPCC, Geneva, Switzerland, 104 pp., 2007.

Klaas, C. and Archer, D. E.: Association of sinking organic matter with various types of mineral

ballast in the deep sea: Implications for the rain ratio, Global Biogeochem. Cy., 16, 63-1–63-14, 2002.
Kleypas, J., Buddemeier, R. W., Archer, D., Gattuso, J.-P., Langdon, C., and Opdyke, B. N.: Geochemical consequences of increased atmospheric carbon dioxide on corals reefs, Science, 284, 118–120, 1999.
Langer, G., Geisen, M., Baumann, K.-H., Kläs, J., Riebesell, U., Thoms, S., and Young, J. R.: Species-specific responses of calcifying algae to changing seawater chemistry, Geochem. Geophy. Geosy., 7, 1–12, 2006.
Montagnes, D. J. S. and Franklin, D. J.: Effect of temperature on diatom volume, growth rate, and carbon and nitrogen content: Reconsidering some paradigms, Limnol. Oceanogr., 46, 2008–2018, 2001.
Redfield, A. C., Ketchum, B. M., and Richards, F. A.: The influence of organism on the composition of seawater, in: The sea, edited by: Hill, N. M., 2nd edn. Wiley, 26–77, 1963.
Reynaud, S., Leclercq, N., Romaine-Lioud, S., Ferrier-Pagès, C., Jaubert, J., and Gattuso, J.-P.: Interacting effect of CO_2 partial pressure and temperature on photosynthesis and calcification in a scleractinian coral, Glob. Change Biol., 9, 1660–1668, 2003.
Riebesell, U., Zondervan, I., Rost, B., Tortell, P. D., Zeebe, R. E., and Morel, F. M. M.: Reduced calcification of marine plankton in response to increased atmospheric CO_2, Nature, 407, 364–367, 2000.
Riebesell, U., Bellerby, R., Engel, A., Fabry, V. J., Hutchins, D. A., Reusch, T. B. H., Schulz, K. G., and Morel, F. M. M.: Comment on "Phytoplankton calcification in a high-CO_2 world", Science, 322, 1466b, doi:10.1126/Science.1161096, 2008.
Rost, B., Zondervan, I., and Wolf-Gladrow, D.: Sensitivity of phytoplankton to future changes in ocean carbonate chemistry: current knowledge, contradictions and research directions, Mar. Ecol.-Prog. Ser., 373, 227–237, 2008.
Schartau, M., Engel, A., Schröter, J., Thoms, S., Völker, C., and Wolf-Gladrow, D.: Modelling carbon overconsumption and the formation of extracellular particulate organic carbon, Biogeosciences, 4, 433–454, 2007, http://www.biogeosciences.net/4/433/2007/.
Sciandra, A., Harlay, J., Lefèbvre, D., Lemée, R., Rimmelin, P., Denis, M., and Gattuso, J.-P.: Response of coccolithophorid *Emiliania huxleyi* to elevated partial pressure of CO_2 under nitrogen limitation, Mar. Ecol.-Prog. Ser., 261, 111–122, 2003.
Smith, S. V. and Key, G. S.: Carbon dioxide and metabolism in marine environments, Limnol.

BGD
6, 11127–11157, 2009

Oceanogr., 20, 493–495, 1975.
Sorrosa, J. M., Satoh, M., and Shiraiwa, Y.: Low temperature stimulates cell enlargement and intracellular calcification of coccolithophorids, Mar. Biotechnol., 7, 128–133, 2005.
Spero, H. J., Bijma, J., Lea, D. W., and Bernis, B. E.: Effect of seawater carbonate concentration on foraminiferal carbon and oxygen isotopes, Nature, 390, 497–500, 1997.
Watabe, N. and Wilbur, K. M.: Effects of temperature on growth, calcification, and coccolith form in *Coccolithus huxleyi* (Coccolithineae), Limnol. Oceanogr., 11, 567–575, 1966.
Yentsch, C. S. and Menzel, D. W.: A method for the determination of phytoplankton chlorophyll and phaeophytin by fluorescence, Deep-Sea Res., 10, 221–231, 1963.
Zeebe, R. E. and Wolf-Gladrow, D.: CO_2 in seawater: equilibrium, kinetics, isotopes, Elsevier Oceanography Series, Elsevier, Amsterdam, 346 pp., 2001.
Zondervan, I., Zeebe, R. E., Rost, B., and Riebesell, U.: Decreasing marine biogenic calcification: A negative feedback on rising atmospheric pCO_2, Global Biogeochem. Cy., 15, 507–516, 2001.
Zondervan, I., Rost, B., and Riebesell, U.: Effect of CO_2 concentration on the PIC/POC ratio in the coccolithophore *Emiliania huxleyi* grown under light-limiting conditions and different daylengths, J. Exp. Mar. Biol. Ecol., 272, 55–70, 2002.

Table 1. Summary of data derived from the culture experiments.

Temperature treatment	13°C						18°C			
CO_2 treatment	Low CO_2		Present CO_2		Future CO_2		Present CO_2		Future CO_2	
pCO_2 (ppm)	180		380		750		380		750	
Duplicate	1	2	1	2	1	2	1	2	1	2
max chl-*a* ($\mu g\,L^{-1}$)	9.8	10.8	9.2	12.4	19.6	15.1	8.4	10.1	10.9	7.3
max cells density (10^5 cell mL^{-1})	2.34	2.34	2.22	2.56	3.84	3.8	6.84	5.20	5.35	4.00
max POC ($mg\,C\,L^{-1}$)	1.85	1.63	1.71	2.09	3.09	2.88	5.16	5.30	4.50	5.52
max PIC ($mg\,C\,L^{-1}$)	4.6	3.98	3.74	5.75	4.53	5.44	5.69	7.45	5.84	6.92
Growth rate, μ (d^{-1})	0.06	0.04	0.04	0.06	0.07	0.08	0.10	0.09	0.07	0.09
Calcification rate ($mg\,C\,L^{-1}\,d^{-1}$)	0.11	0.06	0.06	0.09	0.17	0.17	0.21	0.19	0.13	0.09

BGD
6, 11127–11157, 2009

Table 2. Summary of cell abundance-normalized POC and PIC concentrations as determined by linear regressions $y=ax+b$ for each culture experiments. Duplicate cultures are presented. The Δ[POC]:Δ[cell] ratio was determined during the exponential cell growth phase. The Δ[PIC]:Δ[cell] ratio was determined during the calcification phase when $\Omega_{cal}>1$.

Ratio $\Delta y:\Delta x$	CO_2/T treatment	Δt	a±SD	r^2	n
Δ[POC]:Δ[cell]	Low CO_2/13°C				
(pmol:cell)	1	8–34	0.77±0.13	0.83	9
	2	8–34	0.60±0.02	0.99	6
	Present CO_2/13°C				
	1	8–57	0.55±0.09	0.72	18
	2	8–57	0.57±0.05	0.89	16
	Future CO_2/13°C				
	1	8–33	0.83±0.19	0.87	5
	2	8–33	0.87±0.15	0.87	7
	Present CO_2/18°C				
	1	4–32	0.36±0.04	0.91	8
	2	4–32	0.60±0.04	0.97	10
	Future CO_2/18°C				
	1	4–32	0.42±0.08	0.78	10
	2	4–32	0.94±0.13	0.87	10
Δ[PIC]:Δ[cell]	Low CO_2/13°C				
(pmol:cell)	1	8–52	1.87±0.14	0.92	17
	2	8–52	1.41±0.21	0.71	17
	Present CO_2/13°C				
	1	8–57	1.29±0.19	0.74	18
	2	8–57	1.38±0.28	0.66	15
	Future CO_2/13°C				
	1	14–40	1.04±0.33	0.77	5
	2	14–40	1.06±0.41	0.62	6
	Present CO_2/18°C				
	1	12–43	0.69±0.12	0.85	8
	2	12–43	1.07±0.20	0.8	9
	Future CO_2/18°C				
	1	4–39	0.71±0.09	0.78	12
	2	4–39	0.93±0.14	0.84	11

BGD
6, 11127–11157, 2009

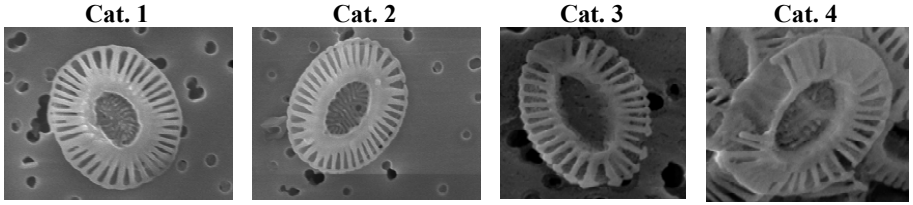

Fig. 1. Scanning electron micrographs of the four categories of coccolith morphology from normal coccoliths (cat. 1) to fragmented coccoliths (cat. 4).

BGD

6, 11127–11157, 2009

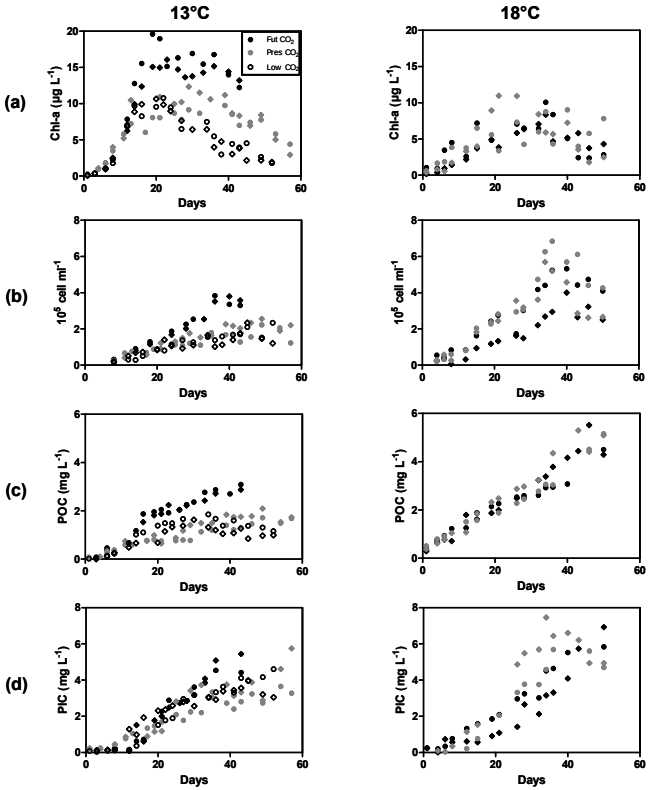

Fig. 2. Evolution with time of **(a)** chl-*a* concentration, **(b)** cell density, **(c)** particulate organic carbon and **(d)** particulate inorganic carbon during the batch culture experiments. Open symbols represent low CO_2 treatment, grey symbols present CO_2 treatment and black symbols future CO_2 treatment. Squares and diamonds represent the duplicate culture experiments. The left panel presents the culture experiments at 13°C and the right one the culture experiments at 18°C.

BGD
6, 11127–11157, 2009

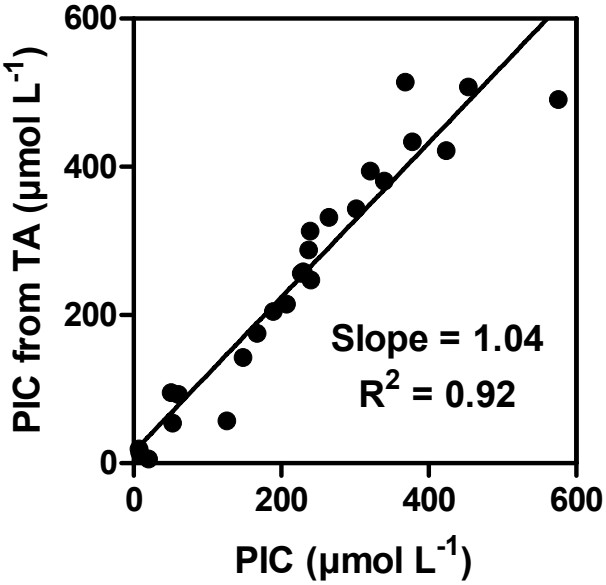

Fig. 3. Correlation between the PIC concentrations deduced from the TA measurement and those measured with a CHN analyzer. Example for the duplicate cultures at future CO_2 and 13°C (n=25, slope=1.042±0.064, r^2=0.92).

BGD

6, 11127–11157, 2009

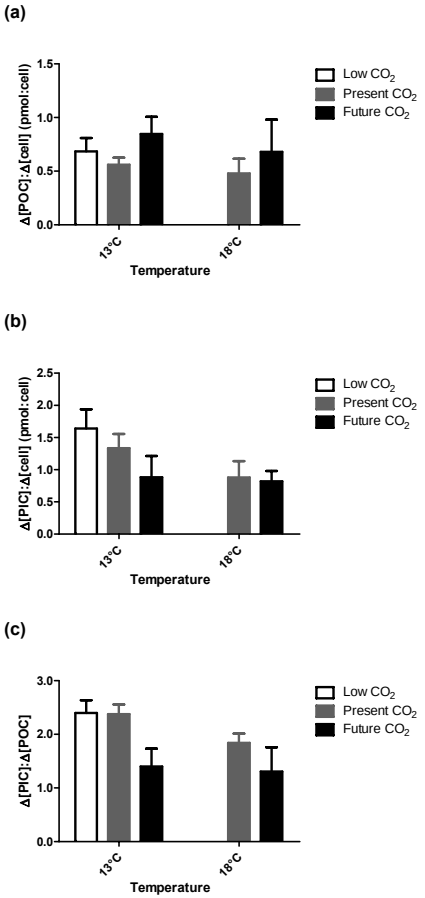

Fig. 4. Concentrations of **(a)** POC and **(b)** PIC normalized to cell abundance during the batch culture experiments. **(c)** PIC:POC ratios for each treatment of pCO_2 and temperature. The standard deviations are also indicated.

BGD
6, 11127–11157, 2009

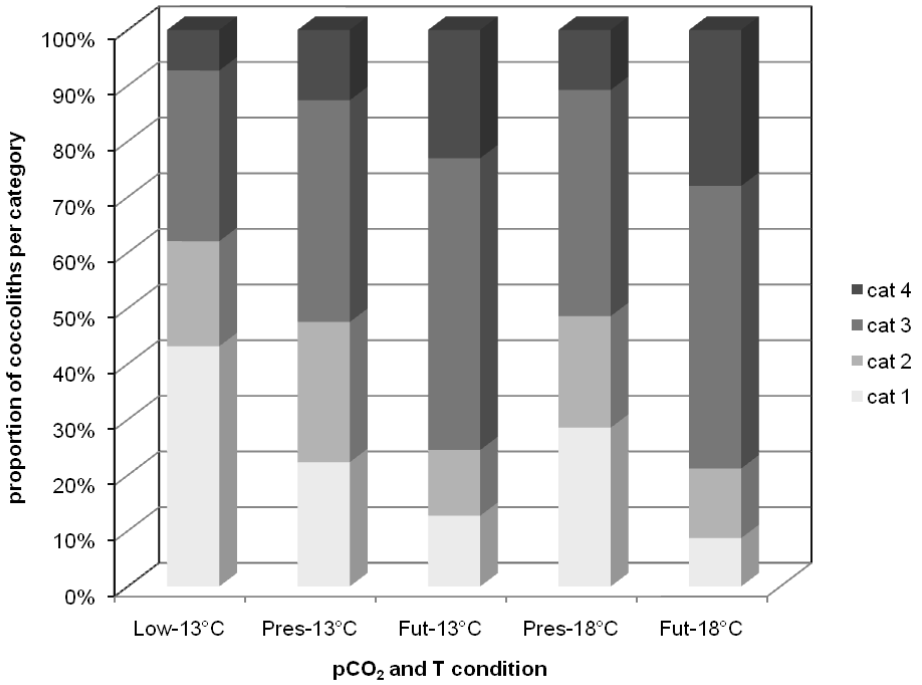

Fig. 5. Percentage of coccoliths per category for each treatment of pCO_2 and temperature.

BGD
6, 11127–11157, 2009

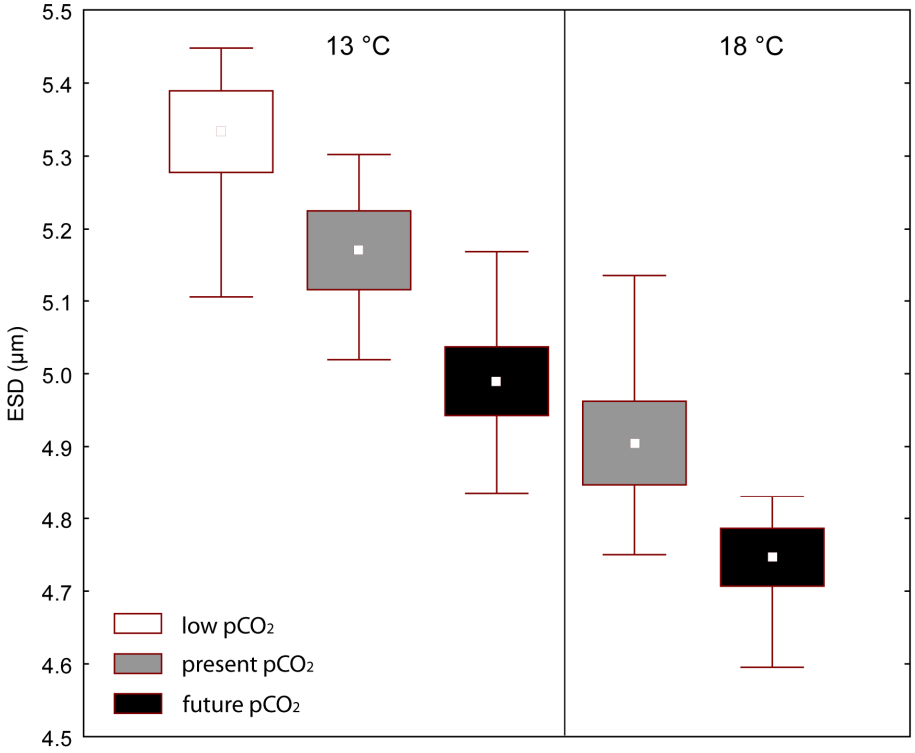

Fig. 6. Mean particle size of CSP for each treatment. The central marker denotes the mean, the standard error is given by the box boundaries, and the whiskers represent the minimum and maximum mean values. The white box represents the low CO_2 treatment, the grey shaded boxes the present CO_2 treatments, and the black boxes the future CO_2 treatments. The right-most two boxes represent the 18°C treatments.

BGD
6, 11127–11157, 2009

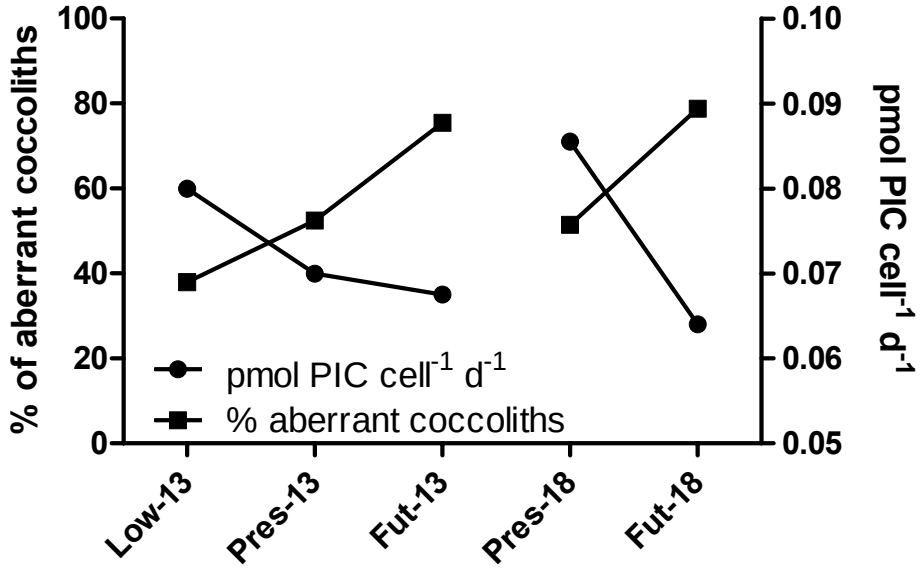

Fig. 7. Percentage of aberrant coccoliths (sum of the category 3 and 4) (solid squares) and production of particulate inorganic carbon per cell and per day (solid circles) per CO_2/temperature treatments.

BGD
6, 11127–11157, 2009